Automatic Right Ventricle Segmentation in CT Images using a Novel Multi-Scale Edge Detector Approach

Sofia Antunes[1,2], Caterina Colantoni[3], Anna Palmisano[3], Antonio Esposito[3], Sergio Cerutti[1], Giovanna Rizzo[2]

[1]Department of Electronics, Information and Bioengineering, Politecnico di Milano, Milan, Italy
[2]Institute of Molecular Bioimaging and Physiology-CNR, Segrate, Italy
[3]Department of Radiology, Scientific Institute H. S. Raffaele, Milan, Italy

Abstract

We present a novel approach for the automatic segmentation of the right ventricle in CT images. We use a level set with a new multi-scale edge stopping function based on spatial oriented filters. This stopping function reduces false edge detection and over-segmentation. The segmentation method was evaluated over 18 CT image studies from healthy and pathologic subjects; results are compared against manual segmentation made by a team of expert radiologists. The mean surface distance error is below 0.64 mm, which proves the effectiveness of the method.

1. Introduction

Segmentation of cardiac images is essential for the diagnosis and follow up of cardiac diseases, as well as to guide surgical interventions [1]. Nowadays, manual delineation of the cardiac cavities from modalities such as computed tomography (CT) or magnetic resonance (MR) is a very difficult task especially for CT due to the huge amount of data that is involved (up to 350 slices for each cardiac phase) [2]. In these cases, an accurate automatic segmentation of the cardiac cavities is highly required for the clinical practice [1].

For the left ventricle (LV) this problem was addressed since long time ago and acceptable results have been already published using different segmentation approaches; a complete review is shown in [1, 3]. However, segmentation of the right ventricle (RV) is still a problem in both CT and MR due to its complex, irregular shape and the high variation among subjects [4]. Most of the existing heart segmentation algorithms that best succeed for CT and MR volumes are based on pre-adapted generic heart templates (parametric shape model), which are fitted to the new volume [1]. However, segmentation based on templates requires training data and an intensive learning process. Moreover, images from pathological subjects are more prone to noise and artefacts, and it could be difficult to capture (new) heavy right ventricle variations mostly present in pathological subjects, because the resulting surface cannot account for great variations on its adaptation towards image boundaries, being limited by the model shape [5].

A wide studied alternative approach for cardiac image segmentation remains boundary driven deformable models based on active contours, where an internal energy term keeps the surface smooth and regular in shape and an external energy term (the stopping function) pushes the curve toward the object frontiers. In particular, Geodesic active contours (GAC) are extensively used since their introduction [6, 7]. However, boundary driven techniques present an important limitation related to the sensitivity of the stopping function to noise [1]. In fact, the main difficulty is the definition of the energy function to drive the curve evolution due to weak boundaries, inhomogeneity and noise commonly observed in medical image.

In this work, we propose an automatic 3D segmentation method based on GAC using a novel optimized stopping function containing spatial oriented filters being able to properly drive the curve evolution. We evaluated this method, acting along a scale space, for the RV segmentation from CT volumes of normal and pathologic subjects to determine its accuracy.

2. Methodology

In this section, we present the framework used to segment the RV. We resampled the volume into the short axis view and, to reduce signal to noise ratio maintaining boundary information, we applied an anisotropic diffusion smoothing [8].

Then we use region-based information to construct the initial segmentation and our new stopping function to attract the curve to the right boundary. A complete

scheme of our approach is shown in Fig. 1. We present the 3D GAC in Sec. 2.1, the construction of the GAC initialization in Sec. 2.2 and in Sec. 2.3 the multi-scale stopping function.

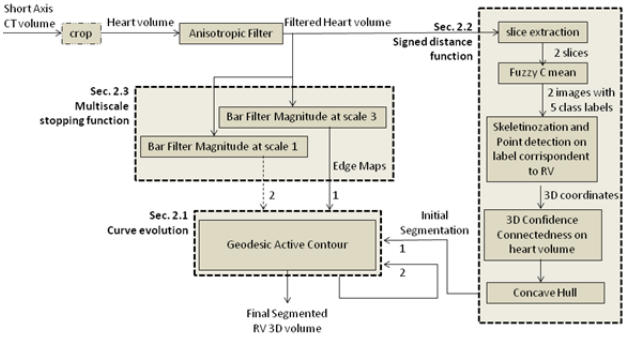

Figure 1. Scheme of the proposed approach. The only manual step is the initial CT volume crop.

2.1. 3D geodesic active contour

GAC consists in integrating curve evolution approaches with classical energy minimization problems, finding a geodesic curve in a Riemannian space derived from the characteristics of the image [6]. Starting from the initial curve, the geodesic flow deforms the contour (evolves) toward the minima, given by a steady state solution. This flow, embedded in a level-set formulation, represents the curve by the zero level set of a higher dimensional function and can be formulated by the following partial differential equation:

$$\phi_t = cg(I)K|\nabla\phi| - bg(I)|\nabla\phi| - a\nabla g \cdot \nabla\phi$$

with K the surface curvature, and where the stopping function g includes a dependence on the curvature term c, the propagation term b, and the advection term a [6]. The use of this implicit, higher dimensional representation addresses the active contour limitations such as the incapability to split objects. GAC has an edge stopping function term g, depending only on the input gray-scale image, that is responsible for attracting the contour towards the boundaries.

2.2. Initialization

We started with the automatic search of coordinates on two slices, at 25% and 50% of the heart volume. We segmented with a Fuzzy C Mean algorithm each of the two slices in 5 labels (Fig. 2a) and identified the label correspondent to the RV (Fig. 2b). After selecting the maximum area structure of this class, we subtracted the dilated LV label to exclude LV and/or miocardium structures (bellow row of Fig.2c). The minimum, maximum and mean from all the detected intersection points of the skeletonization of this segment were used as seed points (Fig. 2d) for a 3D connected confidence region growing algorithm. We summed the segmentations resulting from the growing process of each seed point and applied an alpha shape algorithm to obtain a concave hull of the region [9]. Finally, we computed the signed distance function on this resulting 3D rough segmentation and used it as our GAC initialization (Fig. 3a). Since in end-diastole (ED) the right cavities are connected without physical separation, we identified both right cavities: atrium and ventricle.

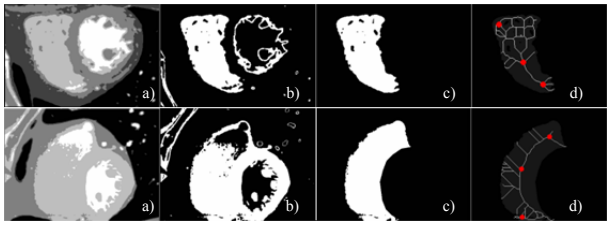

Figure 2. Steps to create the rough initial segmentation shown in two different subjects: a) segmented slice (5 labels), b) label containing RV, c) maximum structure of the correspondent label and subtraction of the dilated LV structure, d) seed points for region growing from the intersection points of the skeletonization of the structure (red points).

2.3. Stopping function

The image-based force that drives the evolution of the active contour is usually based on conventional edge-detectors, such as gradient operator [6, 7] or gradient vector flow [10]. Refinements with the Canny edge detector [11] were introduced, as well as weighted edge-based energy through the entire curve evolution [12]. However, they fail in most cases of medical image segmentation due to blurred or discrete edges[1] and stopping at the right boundary continues to be a very hard task. To enhance the ability for cardiac image segmentation, we introduced here a new stopping function that improved accuracy of the boundary detection.

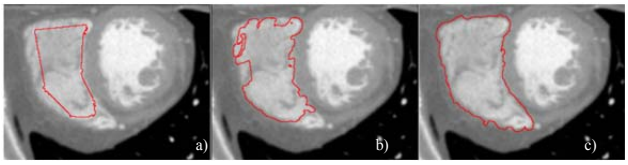

Figure 3. Segmentation steps: from the a) initialization of the level set to b) the first bar filters scale (g_1) until c) second bar filters scale (g_2) of the level set stopping function.

The stopping function consisted in decreasing the image scale space, letting the level set to expand at each step, preventing in this way over-segmentation (Fig. 3).

Multi-scale was performed using the maximum response of two bi-dimensional bar filters (second derivative of a Gaussian filter, characterized by σ_x and σ_y) at 6 orientations, where we decreased the scale (i.e. σ_x and σ_y) from one step to the other [13]. The bi-dimensional bar filters are applied in the three orthogonal plans, and for each voxel, the maximum response was chosen. Our stopping function g has the general form:

$$g_n = \frac{1}{1 + e^{\left(\frac{I * h_n - \beta_n}{0.1}\right)}} \text{ with } n = 1,2$$

where h and β change at each step. h_1 and h_2 are the maximum responses of the two bar filters, with scales (σ_x, σ_y) = (3,9) and (1,3) respectively, and the values of β1 and β2 are 0.1 and 0.05 respectively.

The GAC configuration chosen was tuned on four subjects, identifying the parameter set that gave the best qualitative overlap to manual segmentation: *a*=1, *b*=3, *c*=1.

3. Evaluation of segmentation accuracy

The proposed 3D method was evaluated over 18 CT volumes acquired for clinical diagnosis and follow-up of patients with suspected cardiac problems (8 normal subjects and 10 subjects with ischemic heart disease) in ED phase and voxel size ranging from 0.31 x 0.31 x 0.3mm up to 0.43 x 0.43 x 0.45mm. 30 equal spaced slices were extracted for each heart volume. For all of the 540 slices, RV was manually outlined by an expert radiologist and the segmentation was additionally controlled by other 2 experts. The manual contours are used as ground truth for the automatic segmentation performance validation. We included in this analysis only slices imaging the RV (without parts of the right atrium). We compared segmentation performance of our approach with the ground truth. The reconstruction of the cavity was done using a surface rendering based on a marching cubes algorithm [14]. For the evaluation, we used different metrics, the overlap measure DICE, the average surface-distance (ASD) which locates the closest point on the other surface (two-sided), the maximum surface distance (MSD) and the percentage of the surface points with errors greater than 2 mm. Further, we measured the method's performance, by calculating the error in ED volumes (Δ vol) for manual and automatic contours.

4. Results

The good correspondence between manual and automatic contour detection can be observed in Fig. 4 for qualitative evaluation. Table 1 presents the quantitative results. The DICE value shows that more than 89% of the RV areas are in concordance with the manual one, as well as the surface measure, where the ASD error is 0.68 mm. Further, 10.4% of the points have a distance greater than 2 mm from the manual segmentation, and the MSD is about 8 mm. The healthy subjects always show slightly better segmentation performance than the pathologic ones. However, residual errors were judged acceptable in all cases by the radiologists.

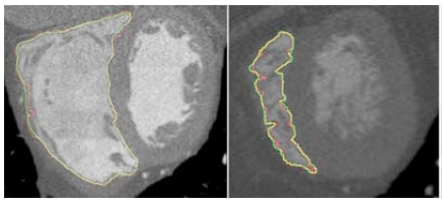

Figure 4. Short axis view for two different subjects and different RV levels; the red contour corresponds to our final segmentation and the green one to the manual drawn ground truth. Yellow corresponds to the overlap of the contours.

Table 1. Quantitative evaluation of the proposed segmentation method (mean±sd). H-healthy,P-pathologic.

	DICE	ASD [mm]	MSD [mm]
H	0.89±0.05	0.60 ± 0.20	8.09±3.40
P	0.90±0.03	0.68 ± 0.26	8.87±2.70

	% > 2mm	Δvol[mm^3]
H	9.46±4.08	8174 ± 3893
P	11.17±5.58	7223 ± 5296

5. Discussion and conclusion

Only heart model based approaches have been proposed for RV segmentation of CT images [2, 15, 16], and this work is the first that obtained good results using only low level information. Despite the objective difficulty of a direct comparison with other state-of-the-art results, due to the use of different datasets, evaluation metrics and ground truth, our results appear to be slightly better than the recently published work. Previous studies [2, 15] reported greater surface distance errors for the RV (1.55 mm and 1.4 mm respectively) than our method (0.68 mm), although the authors used a larger number of subjects. In [16] the authors achieved similar results to ours (surface distance error = 0.63 and % > 2mm = 4.2), however they underestimated the segmentation error, obtaining the ground truth by manually correcting their automatic segmentation. In fact, the main problem we encountered in the validation was the accuracy of the manual segmentation due to the effort required to segment manually a great amount of slices.

In conclusion, we have presented and validated a level

set method with incorporation of a new multi-scale stopping function for segmenting the RV on CT images. To our knowledge, this is the first published approach presenting bar filters on a curve evolution segmentation of the RV, obtaining promising results from a low level based segmentation perspective. Nevertheless, there are further improvements needed; it would be desirable to separate automatically the RV from the right atrium, based on some prior information. Finally, and in order to improve our results, it is essential to evaluate the method on a larger dataset.

Acknowledgements

The work was partially supported by the Italian Ministry of Health GR-2009-1594705. Sofia Antunes is grateful to the Portuguese Foundation for Science and Technology (FCT) by generous funding through the grant SFRH/BD/69488/2010.

References

[1] Kang D, Woo J, Slomka PJ, Dey D, Germano G, Jay Kuo C. Heart chambers and whole heart segmentation techniques: review. Journal of Electronic Imaging 2012; 21: 010901-1.

[2] Zheng Y, Barbu A, Georgescu B, Scheuering M, Comaniciu D. Four-chamber heart modeling and automatic segmentation for 3-D cardiac CT volumes using marginal space learning and steerable features. IEEE Trans Med Imaging 2008; 27: 1668-1681.

[3] Petitjean C, Dacher J. A review of segmentation methods in short axis cardiac MR images. Med Image Anal 2011; 15: 169-184.

[4] Grosgeorge D, Petitjean C, Caudron J, Fares J, Dacher J. Automatic cardiac ventricle segmentation in MR images: a validation study. International Journal of Computer Assisted Radiology and Surgery 2011; 6: 573-581.

[5] Lynch M, Ghita O, Whelan PF. Automatic segmentation of the left ventricle cavity and myocardium in MRI data. Comput Biol Med 2006; 36: 389-407.

[6] Caselles V, Kimmel R, Sapiro G. Geodesic Active Contours. 1995.

[7] Malladi R, Sethian J, Vemuri B. Shape modeling with front propagation - a level set approach. IEEE Trans Pattern Anal Mach Intell 1995; 17: 158-175.

[8] Perona P, Malik J. Scale-Space and Edge-Detection using Anisotropic Diffusion. IEEE Trans Pattern Anal Mach Intell 1990; 12: 629-639.

[9] Edelsbrunner H, Mücke EP. Three-dimensional alpha shapes. ACM Trans Graph 1994; 13(1):43-72.

[10] Paragios N. A variational approach for the segmentation of the left ventricle in cardiac image analysis. International Journal of Computer Vision 2002; 50: 345-362.

[11] Somkantha K, Theera-Umpon N, Auephanwiriyakul S. Boundary detection in medical images using edge following algorithm based on intensity gradient and texture gradient features. Biomedical Engineering, IEEE Transactions On 2011; 58: 567-573.

[12] Appia V, Yezzi A. Active geodesics: Region-based active contour segmentation with a global edge-based constraint. in Computer Vision (ICCV), 2011 IEEE International Conference On 2011; 1975-1980.

[13] Varma M, Zisserman A. A statistical approach to texture classification from single images. International Journal of Computer Vision 2005; 62: 61-81.

[14] Schroeder W, Martin K, Lorensen B. The Visualization Toolkit 2nd edn. Upper Saddle River, NJ: Prentice-Hall, 2002.

[15] Kirisli HA, Schaap M, Klein S, Papadopoulou SL, Bonardi M, Chen CH, Weustink AC, Mollet NR, Vonken EJ, van der Geest RJ, van Walsum T, Niessen WJ. Evaluation of a multi-atlas based method for segmentation of cardiac CTA data: a large-scale, multicenter, and multivendor study. Med Phys 2010; 37: 6279-6291.

[16] Ecabert O, Peters J, Walker MJ, Ivanc T, Lorenz C, von Berg J, Lessick J, Vembar M, Weese J. Segmentation of the heart and great vessels in CT images using a model-based adaptation framework. Med Image Anal 2011; 15: 863-876.

Address for correspondence.

Sofia Antunes
IBFM-CNR
Via Fratelli Cervi 93,
20090 Segrate (Milano), Italy
sofigantunes@gmail.com.